

Mechanical Characterization of Electrostatic MEMS Switches

*F. Souchon¹, A. Koszewski¹, D. Levy¹, P.L. Charvet¹

¹CEA-LETI-MINATEC, Grenoble, FRANCE, f.souchon@cea.fr

ABSTRACT

This paper presents a methodology developed to characterize the mechanical properties of MEMS switches. Mechanical experiments have been performed to explain the electrostatic behavior of an ohmic electrostatic series switch made by CEA-LETI.

The mechanical properties of switches are characterized by nanoindentation experiments : membrane stiffness, gap heights and contact load. These results have been compared to the results obtained by simple analytical models : the mechanical model shows a good correlation with a membrane stiffness currently around 50-100 N/m, and the electrostatic model gives capacitance values in accordance with measurements.

Based on these results, the electrostatic behavior of switches has been analysed : the influence of the mechanical properties on the ohmic and capacitive responses is pointed out.

Keywords: MEMS, switch, nanoindentation, stiffness, model

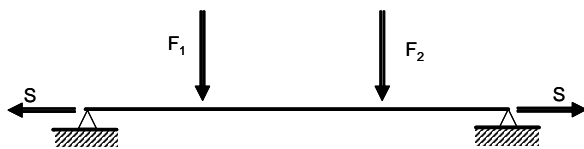
1 INTRODUCTION

Over the past years, CEA-LETI has been developing electrostatic MEMS switches. This paper is focused on the mechanical study that has been performed in order to explain the electrostatic behavior of an ohmic electrostatic series switch. Experimental and theoretical aspects are compared through two types of switches which are different from geometric and process flow standpoints.

2 ANALYTICAL MODEL

2.1 Mechanical model

The switch is modeled as a fixed-fixed beam, with two vertical symmetric loads corresponding to the actuating electrostatic force, and two axial stretching forces corresponding to the effect of the residual stress (see Fig. 1).



S : axial force / F_1, F_2 : vertical force

Figure 1 : Mechanical model of the switch

The analytical model is derived using the classic formula as described in reference [1].

(1) is the final equation used to calculate the stiffness of the MEMS switch.

$$k = \frac{F_1 + F_2}{z(d_1) + z(d_2)} \quad (1)$$

where

$$z(d_1) = -\frac{F_1 \sinh pd_1}{Sp \sinh pl} \sinh px + \frac{F_1 d_1}{Sl} x + \frac{M_{01}}{S} \left[1 - \frac{\cosh p \left(\frac{l}{2} - x \right)}{\cosh \frac{pl}{2}} \right] \quad (2)$$

and

$$M_{01} = F_1 \left(\frac{2Elu}{l \tanh u} \right) \left(\frac{\sinh pd_1}{S \sinh pl} - \frac{d_1}{Sl} \right) \quad (3)$$

and $p^2 = \frac{S}{EI}$, $u = \frac{pl}{2}$, $I = \frac{wt^3}{12}$, k is the membrane stiffness, F_n is the n^{th} vertical load, z is the deflection of the beam, d_n is the distance from the anchor to the n^{th} vertical load, M_0 is the force moment in the anchor, S is the axial force due to residual stresses, w is the width of the beam, t is the thickness of the beam, l is the length of the beam, E is the Young's modulus.

2.2 Electrostatic model

The actuator's equivalent capacitor is modeled by 2 capacitors in parallel. Each capacitor between symmetric electrodes and coplanar wave guide can be considered as a parallel plate capacitor [2].

Based on these hypothesis, the capacitance of the switch is simply expressed by the following formula (4) :

$$C = \frac{2\epsilon_0 A}{y_e + \frac{t_d}{\epsilon_r}} \quad (4)$$

where C is the actuator capacitance, ϵ_0 is the vacuum permittivity, ϵ_r is the relative dielectric constant, A is the electrode surface, t_d is the dielectric thickness, y_e is the air gap between electrodes.

The capacitances for up-state position and down-state position can be easily calculated from equation (4).

3 SWITCH DESCRIPTION

3.1 Design and process flow

The ohmic electrostatic switch was designed for RF applications and implemented on a coplanar wave guide using full wave analysis [3].

The series switch (see Fig. 2) is made of a silicon nitride fixed-fixed membrane with patterned metallic contacts: 2 symmetrical electrodes located inside the membrane actuate the membrane while a center metallic contact with 2 dimples short-circuits the transmission line.

When a biasing voltage is applied between the electrodes and the coplanar wave guide ground plans, the membrane is pulled down and the transmission line is short-circuited by the metallic contact.

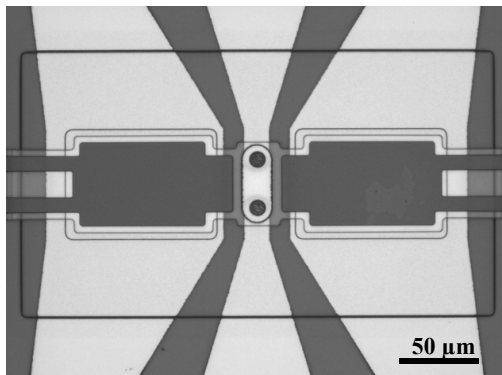


Figure 2 : Top view of a fabricated ohmic electrostatic series switch

The main steps of the switch fabrication process are as follows (see Fig. 3) :

- After a thermal oxidation on a silicon wafer, 2 etching steps are required to create a cavity with bumps,
- A gold layer is deposited and patterned to define coplanar wave guide and RF lines,
- A thick photo resist sacrificial layer is deposited by means of spin coating and then patterned,
- A first silicon nitride layer is deposited, followed by a TiN layer for electrodes. This last layer is patterned before being covered with a second silicon nitride layer,
- The switch contact is then realized by a nitride etching and a gold layer deposition. A last silicon nitride layer is deposited,
- The process ends with pads and membrane opening, and with removal of the sacrificial layer in dry oxygen plasma.

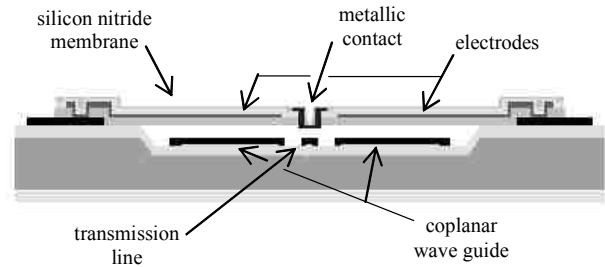


Figure 3 : Schematic stack of the ohmic electrostatic series switch

3.2 Type description

Various types of switches have been designed and manufactured. Each one is different from geometric and process flow standpoints.

This paper presents the results achieved for 2 types of switches among these : A-type and B-type. The 2 types of switches come from 2 runs of fabrication with geometrical design and process flow variations. The main differences are listed below :

- A longer beam for B-type switches,
- A lower residual stress in the membrane for B-type switches,
- Different etching depths to get a bigger electrode gap and a smaller contact gap for A-type switches
- 2 different process flows to realize the switch contact, in particular to etch the silicon nitride and the sacrificial layer before the gold layer deposition.

4 EXPERIMENTAL SET-UP FOR MECHANICAL CHARACTERIZATION

The mechanical properties of the switches have been characterized by nanoindentation experiments. The experiments consist in applying a vertical concentrated load to the indenter tip and measuring the force and the displacement. More precisely, the stiffness of the contact between the indenter tip and the beam is continuously measured by superimposing simultaneously an oscillating force, and the test is automatically stopped as soon as the stiffness rises above a limit value in order to keep the switch working.

In practice, nanoindentation experiments have been performed at the membrane center and at the electrode center in order to measure the membrane stiffness and two gap heights: the contact gap between dimples and transmission line, and the electrode gap between the electrodes. The contact load required for getting the ohmic switching have been also extracted from experiments made at the membrane center.

5 RESULTS AND DISCUSSION

5.1 Mechanical behavior

The A-type switch has a usual mechanical behavior as shown in Figure 4 (effective stiffness versus the indent displacement). The membrane center stiffness presents usually a step which corresponds to the membrane free stiffness before the dimples of the metallic contact and the transmission line get into contact. The electrode center stiffness presents 2 steps: one before and another one after contact at the membrane center. The stiffness is respectively around 110N/m at the membrane center, 130 N/m at the electrode center before the contact at the membrane center and 200 N/m after contact. As wanted, the contact gap height is very small compared to the electrode gap height : 130 nm against 650 nm.

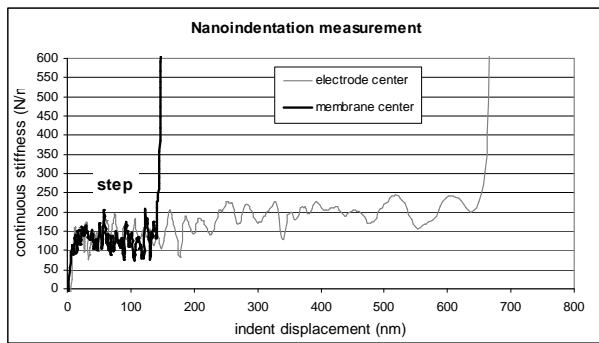


Figure 4 : Nanoindentation measurement A-type switch

The B-type switch does not have the same behavior (see Fig. 5). The membrane center stiffness presents an additional step. The first step corresponds to the membrane free stiffness, the additional step could correspond to a 2 phase contact between the dimples of the metallic contact and the transmission line.

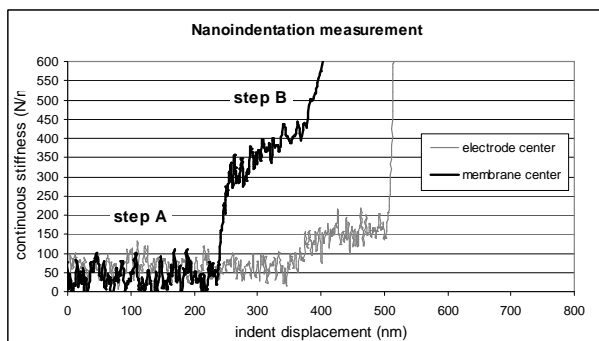


Figure 5 : Nanoindentation measurement B-type switch

These hypothesis have been confirmed by a failure analysis. Various investigations show that the dimples surface is significantly different between the 2 types of switches. Figures 6 and 7 present SEM observations for the

2 switches. The dimples for the A-type have a rough and quite homogeneous surface. Comparatively, B-type switches are less homogeneous with higher peaks which can explain the stiffness trend : after the first contact of the highest peak of 2 dimples on the transmission line, the membrane could twist to put the second dimple in contact. The process flows used to make the switch contact explain these differences between the dimples of the 2 switches.

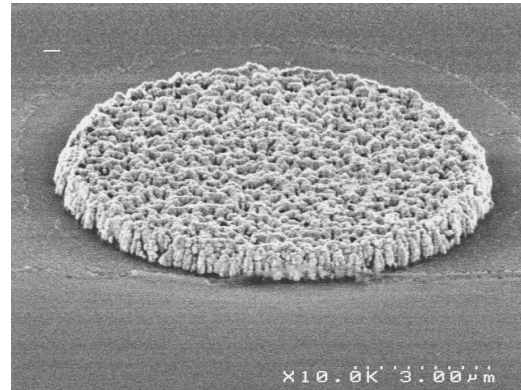


Figure 6: SEM observation of membrane dimple surface _ A-type switch

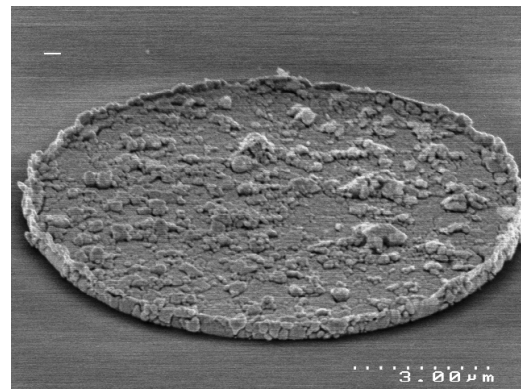


Figure 7: SEM observation of membrane dimple surface _ B-type switch

The free stiffness of B-type switches at the membrane center is around 50 N/m, the stiffness after initial contact is very high between 300 and 500N/m. The classical behavior at the electrode center is similar to the A-type switch with 2 steps : one before and another one after contact at the membrane center, the value are respectively 60 N/m and 160 N/m. The contact gap is a little bit smaller than the electrode gap, respectively 430 and 480 nm.

The contact load required to get the ohmic switching is significantly higher for the B-type switch. This is due to a higher contact gap height and the additional step with a higher stiffness compared to A-type switches.

Table 1 summarizes the mechanical experimental results obtained on the 2 types of switches where K1 is the free stiffness at the membrane center, K2a is the free stiffness at

the electrode center, K2b the stiffness at the electrode center after contact at the membrane center, Gc the contact gap height, Ge the electrode gap height, Fc the necessary load for contact switching.

	Stiffness (N/m)			Gap Height (nm)		Load (μ N)
	K1	K2a	K2b	Gc	Ge	Fc
A-type	110	130	200	130	650	14
B-type	50	60	150	420	480	58

Table 1 : Mechanical experimental results

The mechanical model detailed in 3.1 has been adapted to fit the nanoindentation experiments (one vertical concentrated load instead of 2). Table 2 presents the experimental and analytical results, and show that the stiffness calculated with the model correlates quite well with the nanoindentation data when the switch behavior is usual.

	Experimental stiffness (N/m)			Analytical stiffness (N/m)		
	K1	K2a	K2b	K1	K2a	K2b
A-type	110	130	200	101	135	214
B-type	50	60	150	48	64	103

Table 2 : Experimental and analytical results for the membrane stiffness

5.2 Electrostatic behavior

The behavior of the 2 switches (see Fig. 8 and 9) have been identified using a classic single sweeping test and illustrates how the 2 gap heights and the contact load manage the electrostatic behavior.

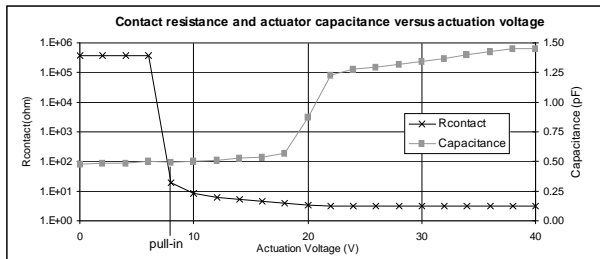


Figure 8 : Single sweeping test A-type switch

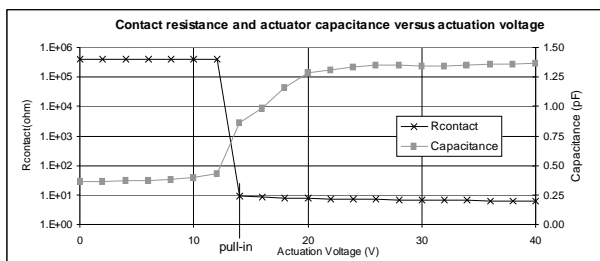


Figure 9 : Single sweeping test B-type switch

The A-type switch has a significant shift between the ohmic and capacitive responses due to the different gap heights.

The B-type switch has no significant shift between the 2 responses due to similar gap heights. And, the ohmic pull-in voltage is bigger for B-type switches due to the contact load and the relative gap heights.

Tables 3 and 4 summarize the electrostatic results obtained on the 2 types of switches where Cup is the capacitance of the actuator in the up-state position, Cdn the capacitance of the actuator in the down-state position for contact switching, $\Delta C = C_{dn} - C_{up}$, Cfull_dn the capacitance of the actuator for electrodes in contact, Vpull-in the actuator voltage for contact switching.

The capacitances have been calculated by using the gap heights given by the nanoindentation experiments; the results given by the analytical model are close to the experimental data for the 2 types of switches.

	Experimental capacitance (pF)				Voltage (V)
	Cup	Cdn	ΔC	Cfulldn	Vpull-in
A-type	0,45	0,48	0,03	1,30	8
B-type	0,33	1,00	0,67	1,38	14

Table 3 : Experimental electrostatic results

	Analytical capacitance (pF)			
	Cup	Cdn	ΔC	Cfulldn
A-type	0,16	0,19	0,03	1,45
B-type	0,21	0,95	0,73	1,45

Table 4 : Analytical electrostatic results

6 CONCLUSION

The paper presents nanoindentation experiments in order to characterize the mechanical properties of MEMS switches : membrane stiffness, gap heights and contact load. These results have been compared to the results given by simple analytical models : mechanical and electrostatic models show a good correlation with experimental data. Finally, the electrostatic behavior of switches are well-understood thanks to these mechanical characterizations.

REFERENCES

- [1] S. Timoshenko, "Strength of Materials, Part I and Part II", 3rd edition, Krieger Publishing Company, 1983, 1010 pages
- [2] G. Rebeiz, "RF MEMS: theory, design and technology", Willey Inter Science Publisher, New Jersey, 2003, 512 pages
- [3] D. Mercier et al., "A DC to 100 GHz high performance ohmic shunt switch", Microwave Symposium Digest, IEEE MTT-S International Volume 3, 6-11 June 2004 pp. 1931-1934